Rev. Mexicana Astron. Astrof., 13, 15-25 (1986)

LOW DENSITY IONIZED GAS ASSOCIATED WITH M17, G333.3 – 0.4 AND RCW 74

I.N. Azcárate[1], J.C. Cersosimo[1], and F.R. Colomb[1]

Instituto Argentino de Radioastronomía
Argentina

Received 1985 August 6

RESUMEN

Se realizaron observaciones en la línea H166α y el continuo a 1.4 GHz en diferentes posiciones en el gas ionizado extendido, asociado a las regiones H II, M17, G333.3 – 0.4, y RCW 74, respectivamente. Se obtuvieron temperaturas electrónicas y otros parámetros físicos de estas regiones y se les comparó con los obtenidos por otros autores a partir de observaciones de líneas de recombinación en radio de más alta frecuencia. Los resultados son compatibles con una descripción de las regiones H II relativamente extendidas, como compuestas por una pequeña región compacta (N_e = 100-1000 cm^{-3}), rodeada de una envoltura de gas ionizado de más baja densidad ($N_e \cong$ 1-10 cm^{-3}). Las temperaturas electrónicas parecen variar con la densidad, al menos en M17.

ABSTRACT

We made observations in the H166α line and in the 1.4 GHz continuum at several positions in extended ionized gas associated with the H II regions M17, G333.3 – 0.4, and RCW 74, respectively. We derived electron temperatures and other physical parameters of these regions and compared them with those obtained by other authors from higher frequency radio recombination line observations. The results are compatible with a description of relatively extended H II regions, each consisting of a small compact region (N_e = 100 to 1000 cm^{-3}) embedded in a extended ionized gas envelope of lower density ($N_e \cong$ 1-10 cm^{-3}). Electron temperatures appear to vary with density, at least in M17.

Key words: INTERSTELLAR MATTER — NEBULAE-H II REGIONS — RADIO RECOMBINATION LINES

I. INTRODUCTION

The H166α line has been observed along the galactic plane for $|l| < 50°$ (Lockman 1976; Hart and Pedlar 1976; Hart *et al.* 1983). This line emission correlates well with the CO emission at 115 GHz, both in distribution and in velocities, (Robinson *et al.* 1984). As is well known, CO is a primary tracer of H_2 in giant molecular clouds. The close association found between giant molecular clouds and H166α emission suggest that this is a good indicator of star formation regions.

The purpose of this paper is to study the H166α emission from the low density and extended ionized gas regions associated with the H II regions M17, G333.3 – 0.4, and RCW 74. To this end we report observations of the three nebulae. M17, G333.3, and RCW 74, have been observed previously at other radio recombination lines, in the radio continuum at different frequencies, in some molecular lines (CO, H_2CO, OH, etc.) as well as at optical wavelengths.

Let us consider first M17. This region has been studied in a large number of radio recombination lines with frequencies ranging from 408 MHz to 88.5 GHz (Goudis 1976), in the optical range and radio lines of CO, H_2CO, OH, H_2O. Molecular line studies of the associated molecular cloud to the small and dense central region have been published by Lada, Dickinson, and Penfield (1974); Lada (1976); Elmegreen and Lada (1976), and Thronson and Lada (1983). H_2O and OH masers toward M17 have been discussed by Knowles, Caswell, and Goss (1976) and Genzel and Downes (1977). H_2CO in absorption was observed by Whiteoak and Gardner (1974), and Downes *et al.* (1980) at velocities (LSR) 23.7 and 23.5 km s^{-1}, respectively (throughout this paper all velocities are referred to the Local Standard of Rest). In CO the velocity is 20 km s^{-1} (Lada *et al.* 1974), and in H_2O it is 19 km s^{-1} (Genzel and Downes 1977). Excited OH emission velocity is 21 km s^{-1}, according to Knowles *et al.* (1976). In general, molecular line velocities agree with recombination line velocities.

The optical observations of [O III] (λ = 5007 A) made by Elliot and Meaburn (1975) show single, double and quadruple profiles, indicating the very complex kinematics of the region, with probably unusual large scale internal motions produced by ionization fronts eating into the adjacent neutral material (Meaburn 1977).

Most of the radio recombination line observations made generally at frequencies $\geqslant$ 5 GHz and with anten-

1. Member of the Carrera del Investigador Científico y Tecnológico del Consejo Nacional de Investigaciones Científicas y Técnicas (*CONICET*), Argentina.

na beams $< 4'$, in the direction of the center of the nebula (G15.0 −0.7), show a single profile. Exceptions are the H76α observations of Gull and Balick (1974) and McGee and Newton (1981), showing double profiles. The H252α observations of Batty (1974), show a difference of 12 km s^{-1} in radial velocities as compared with higher frequency observations.

The region centered at galactic coordinates l = 333.3°, b = −0.4° (we shall call it G333.3) has been observed in H109α, H76α, H90α, and in molecular lines from H_2CO, OH and CO. Observations of CO (J = 1→0) were made by Gillespie *et al.* (1977). The transition CO (J=2→1) has been studied with more detail by De Graauw *et al.* (1981) in the associated molecular cloud. H_2CO was observed in absorption by Whiteoak and Gardner (1974). Molecular line velocities are in general ≃ −51 km s^{-1}, in good agreement with recombination line velocities.

RCW74 (G305+4, 0.2) has been observed in the H109α, H76α, H252α lines, CO (Gillespie *et al.* 1977; Brand *et al.* 1984), H_2CO (Whiteoak and Gardner 1974), and OH. Molecular line velocities fall in the range −35 km s^{-1} to −40 km s^{-1}. Recombination line velocities are ≃ −40 km s^{-1}.

We shall describe in the next section observation carried out of the H166α line and 1.4 GHz continuum, which seem to prove the existence of extended emission regions embedding the three nebulae.

II. OBSERVATIONS

a) *The Line*

The observations were made with the 30-meter diameter antenna of the Instituto Argentino de Radioastronomía. The noise temperature of the system was about 85 K for a cold sky background and the half-power beam-width (HPBW) was 34 arcmin at 1420 MHz. The frequency-switching technique was used for the observations. The back-end included a filter bank of 112 filters of 10 kHz widths. These gave a velocity resolution of 2 km s^{-1}. We observed 9 positions for each H II region, at a separation of 0.5°. The total integration time was about four hours for each position. This resulted in an 'rms' noise of 0.025 K. The final profiles were obtained by removing the instrumental baselines using in most of the cases a second order polynomial.

b) *The Continuum*

The three nebulae were observed in the continuum at 1420 MHz by making several right ascension scans spaced 0.5° in declination. The continuum receiver covered a bandwidth of 40 MHz centered at 1420 MHz. A filter of 2MHz bandwidth centered at 1420.4057 MHz was used to eliminate the emission from galactic neutral hydrogen. The receiver was operated in the Dicke switching mode. The velocity of the right ascension scans was 0.5ᵘ minute.

III. RESULTS

a) *Structure of M17*

The galactic coordinates and some parameters of the observed profiles are given in Table 1. Some of the profiles are shown in Figure 1. The central profile, as well as several other ones, have centroid velocities of 20 km s^{-1}. Other profiles, as the one at l = 14.5°, b = 0.0°, have centroid velocities of 35 km s^{-1}. This would mean that emission has originated (for that profile, according to the Schmidt rotation model), from more distant regions along the line of sight. The FWHM (Full-Width-Half-Maximum) is 35 km s^{-1} for most of the profiles.

TABLE 1

PARAMETERS CALCULATED FOR DIFFERENT OBSERVED POINTS IN M17

ℓ (°)	b (°)	$\int T_L\, dv$ (K km s^{-1})	T_C (K)	T_e^* (K)
14.5	0.0	7.364	8	3251 ± 300
14.5	− 0.5	3.092	8	6900 ± 700
15.5	0.0	0.578	8	–
14.5	− 1.0	1.792	14	–
15.5	− 1.0	4.856	11.6	6450 ± 650
15.5	− 0.5	5.108	20	10000 ± 100
15.0	− 1.0	11.140	26	6300 ± 600
15.0	− 0.7	25.453	38	4300 ± 400
15.0	0.0	2.204	4	5000 ± 500

The continuum map of the observed region is shown in Figure 2. The numbers at the contour levels correspond to degrees Kelvin of antenna temperature. The positions given in Table 1 are shown by X marks. The values of the continuum antenna temperatures T_c, given in the map and the integrated power $\int T_L\, dv$ under the corresponding H166α profiles, were used to derive electron temperatures T_e (cf. Table 1). The values of T_e obtained in this way range from 3000 to 12000 K.

The integrated flux density from the region associated with M17 is 675 Jy. Using this value and according to a very simplified model of a spherical H II region with uniform electron temperature and density given by Schraml and Mezger (1969), we computed an rms electron density ≅ 12 cm^{-3} and obtained a value of emission measure of 1.04×10^4 pc cm^{-6}. The adopted distance is 2.3 kpc and the diameter of the spherical model is D ≅ 50 pc.

Higher frequency observations in the direction of G15.0, −0.7, which is the center of the observed region (Wilson *et al.* 1970; McGee and Newton 1981; Downes *et al.* 1980) show density and emission measure values about two orders of magnitude greater than our values (see Table 2). This difference can be explained by the

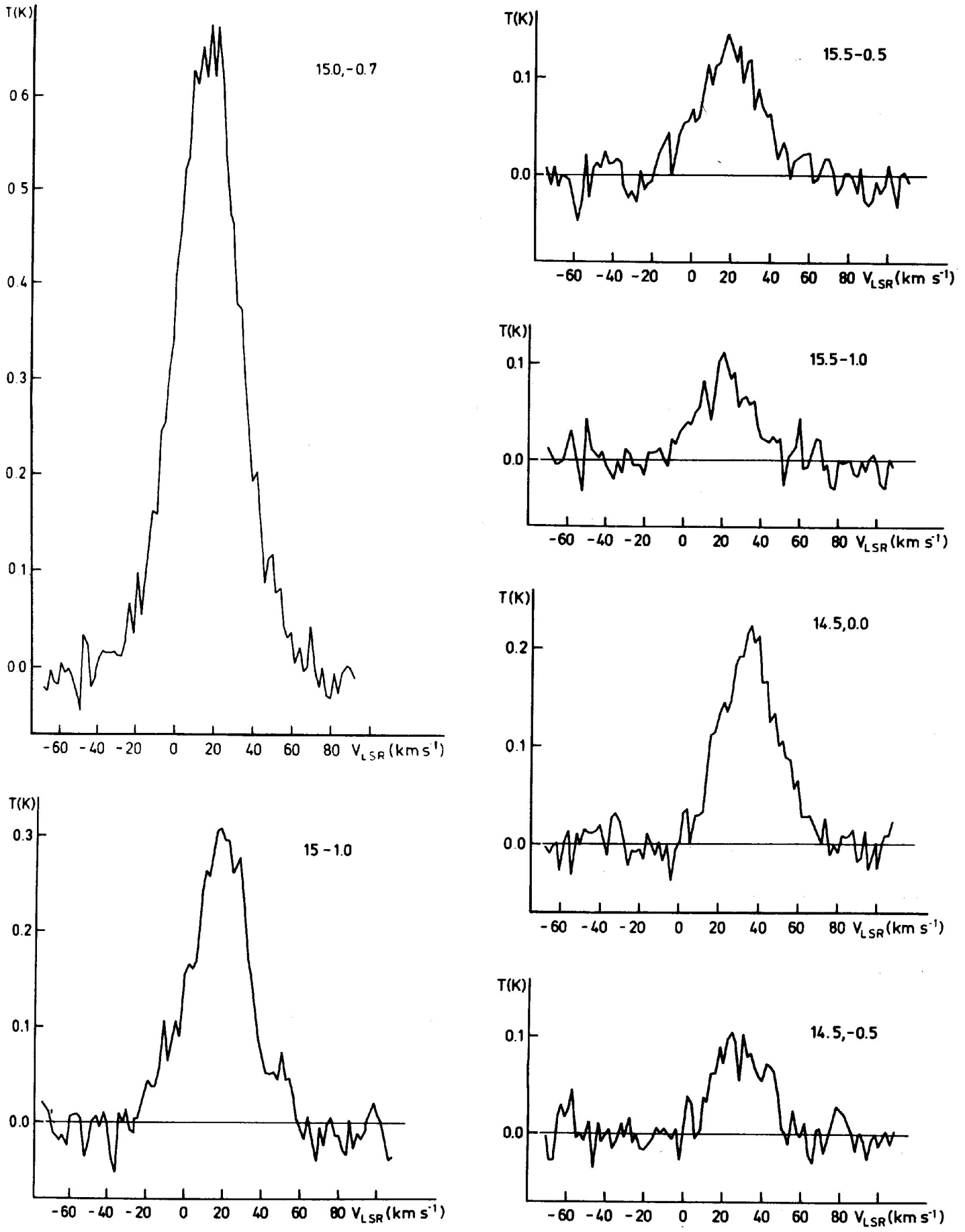

Fig. 1. Some profiles obtained from the H166α observations of the M17 region.

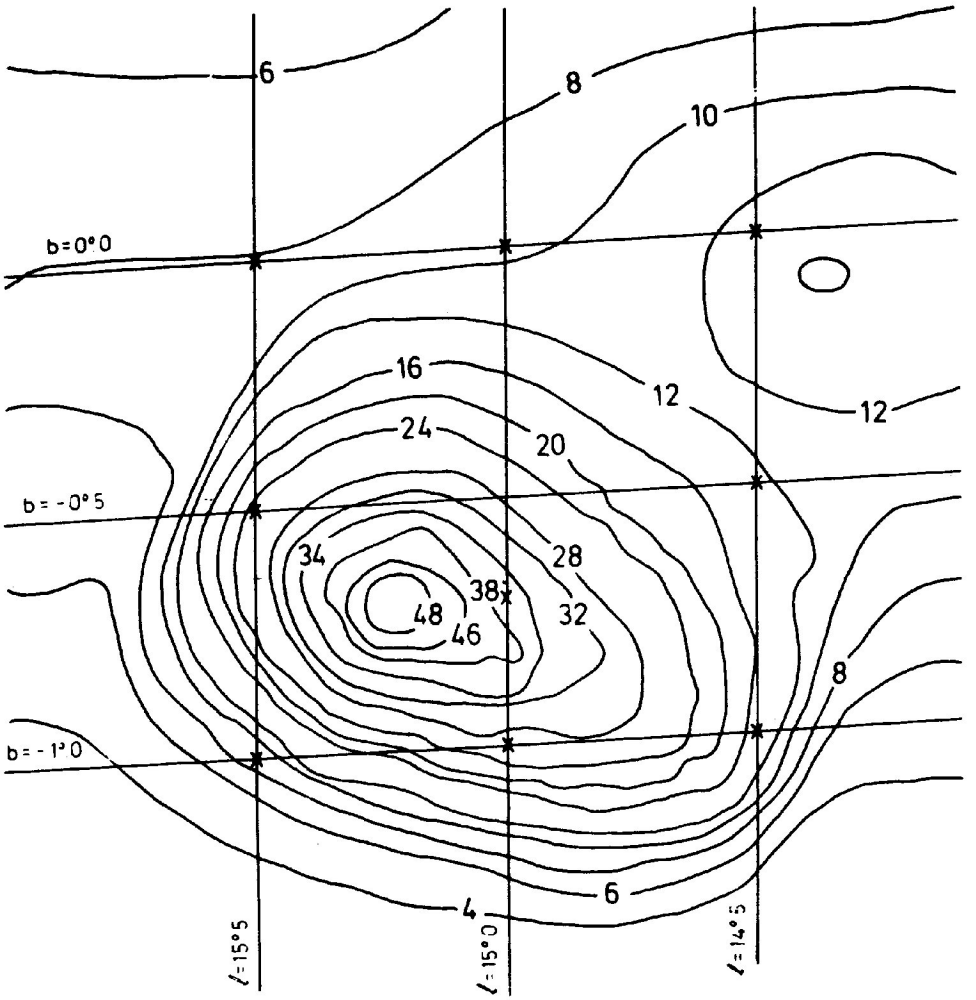

Fig. 2. Continuum map at 1420 MHz of the region associated with M17. The crosses indicate the positions where the H166α observations were made.

TABLE 2

PHYSICAL PARAMETERS OBTAINED FROM DIFFERENT RECOMBINATION LINE OBSERVATIONS FOR M17, G333.3 AND RCW 74

	M17			G333.3			RCW 14		
Reference	EM (pc cm^{-6})	N_e (cm^{-3})	T_e (K)	EM (pc cm^{-6})	N_e (cm^{-3})	T_e (K)	EM (pc cm^{-6})	N_e (cm^{-3})	T_e (K)
Wilson *et al* (1970) H109α	1.6×10^6	594	6200	2.1×10^6	994	5000	5.1×10^5	223	5200
Downes *et al* (1980) H110α	1.6×10^6	–	9100	–	–	–	–	–	–
McGee and Newton (1981) H76α	3×10^6	1010	8300	7.5×10^5	456	7400	7.2×10^5	456	6900
Our observations (1984) H166α	1.04×10^4	12	5500	8.5×10^3	7	5200	8.81×10^3	5	4500

fact that at the frequency of the H166α line and with our antenna beam, the observations are most sensitive to the extended and diffuse parts of the nebula, the compact and higher emission measure regions near the center becoming optically thick at 1.4 GHz and suffering greater beam dilution.

b) *Electron Temperatures*

The electron temperatures were derived from the observed H166α profiles by using the line to continuum ratio technique. The formula used was:

$$\frac{\int T_L\, dv}{T_c} = \frac{7440}{a(\nu, T_e)} \frac{1}{1+(N(He^+)/N(H^+))} \times \left(\frac{\nu}{GHz}\right)^{1.1} \left(\frac{T_e^*}{K}\right)^{-1.15} \quad (1)$$

where T_e^* is the electron temperature if the emission levels are in Local Thermodynamical Equilibrium (LTE), $a(\nu, T_e)$ is a factor close to unity, tabulated by Mezger and Henderson (1967), ν is the line frequency in GHz, $N(He^+)/N(H^+)$ is the number density ratio of ionized helium to ionized hydrogen generally assumed to be 0.1, $\int T_L\, dv$ is the integral power under the line (in K km s^{-1}) and T_c is the continuum antenna temperature.

If it is assumed that T_e is constant over the whole region, then $\int T_L\, dv$ should be proportional to T_c. In Figure 3, we have plotted $\int T_L\, dv$ against T_c. A least squares straight-line fit to the observed points, excluding those corresponding to $\ell = 14.5°$, $b = -1.0°$, $\ell = 15.5°$, $b = 0.0°$ (very noisy profiles), results in a slope which corresponds to $T_e = 4800 \pm 480$ K. This method has been used by other authors (Jackson and Kerr 1975; Hart and Pedlar 1976) to estimate the electron temperature in the presence of non-thermal continuum uniformly distributed over the whole source. The electron temperature computed in this way, is independent of the non-thermal continuum emission. This should be the case with the general non-thermal galactic continuum emission.

By looking at Figure 3, it can be seen that the fitting by a straight line is not very satisfactory, in particular for the data corresponding to the position of galactic coordinates $\ell = 15.5°$, $b = -0.5°$ ($\int T_L\, dv = 5.108$ K km s^{-1}, $T_c = 20$ K). That would indicate that the non-thermal contribution in that direction is greater than at the other points, that is to say there would be contributions to the continuum along this particular line of sight, from regions without H166α emission. However, the correlation coefficient (0.8934), estimated by using the 't' Student distribution (Moroney 1951), suggests that the correlation is significant.

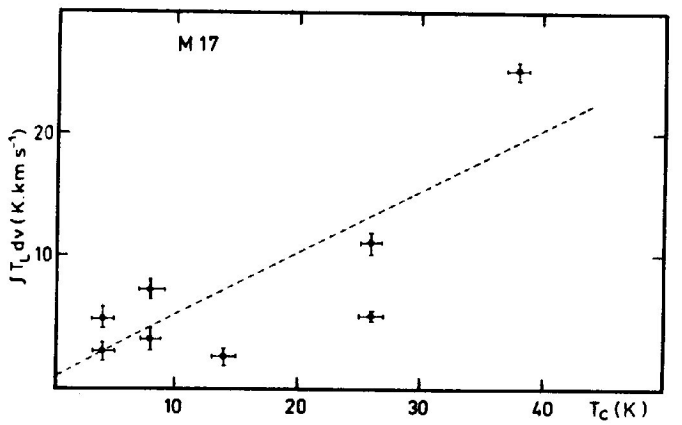

Fig. 3. $\int T_L\, dv$ versus T_c for M17. The dashed line corresponds to the least squares straight-line fit to the observational results.

On the other hand, the mean value of T_e^* obtained from the individual profiles, excluding the position at $\ell = 15.5°$, $b = -0.5°$ (cf. Table 1) is $T_e^* = 5400$ K. This value is not very different from the one obtained by means of the statistical method considered above. Therefore, we can assume that an average value of 5000 K as a first approximation is a good estimate for the electron temperature of the low density ionized gas ($N_e \simeq 12$ cm^{-3}) associated with M17.

b) *G333.3*

The galactic coordinates and other parameters of the observed profiles are shown in Table 3. Some of the profiles are shown in Figure 4. The centroid velocities of the profiles are $\simeq -50$ km s^{-1}, having a FWHM of 30 km s^{-1}. The asymmetry of some profiles, given by the possible presence of a component at more negative velocities, could be due to ionized gas at a larger distance than the H II region we are studying.

TABLE 3

PARAMETERS CALCULATED FOR DIFFERENT OBSERVED POINTS IN G333.3

ℓ (°)	b (°)	$\int T_L\, dv$ (K km s^{-1})	T_c (K)	T_e^* (K)
333.3	− 0.4	12.18	26	5800 ± 600
334.0	− 0.5	1.722	8	1000 ± 1000
334.0	0.0	2.718	10	9400 ± 900
333.5	0.0	5.860	14	6450 ± 650
334.0	− 1.0	1.354	4	7760 ± 800
333.0	− 1.0	2. 714	10	9400 ± 900
333.5	− 1.0	1.818	5	7290 ± 700
333.0	0.0	5.426	12	6000 ± 600
333.0	− 0.5	12.88	26	5600 ± 500

The continuum map is shown in Figure 5. The positions where the line was observed are shown by crosses. The values of electron temperatures for each position are given in Table 3 and range from 6000 to 11000 K. The integrated flux density for the extended region associated to G333.3 of about 2° of diameter is 1500 Jy. Under the same simplified assumptions made for M17 (uniform electron temperature and density) we computed a rms electron density $\simeq 7$ cm^{-3} and a value for the emission measure of 8.10^3 pc cm^{-6}. The adopted distance is 3.9 kpc and the diameter of the spherical model is $D \simeq 129$ pc.

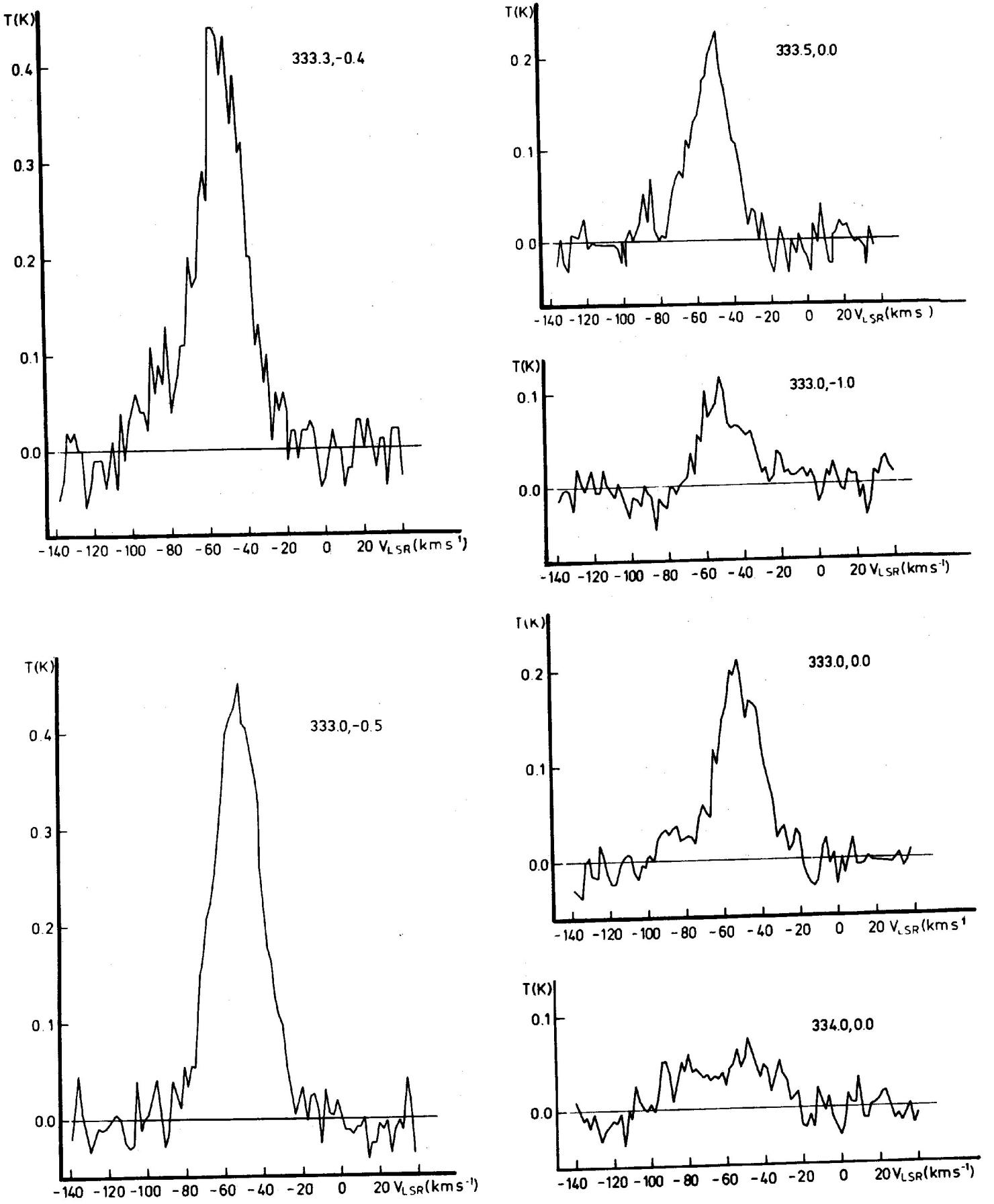

Fig. 4. Some profiles obtained from the H166α observations of the G333.3 region.

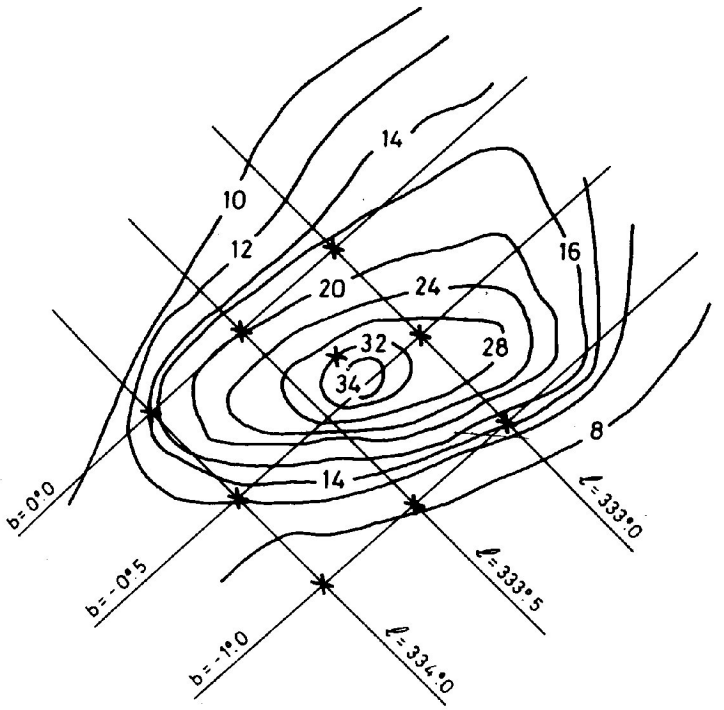

Fig. 5. Continuum map at 1420 MHz of the region associated to G333.3 The crosses indicate the positions where the H166α observations were made.

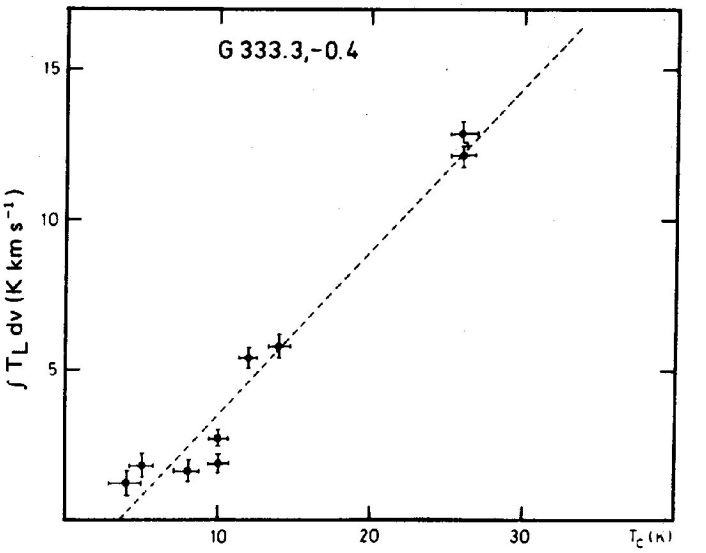

Fig. 6. $\int T_L\,dv$ versus T_c for G333.3. The dashed line corresponds to the least squares straight-line fit to the observational results.

As in the case of M17, higher frequency radio recombination line observations in the direction of G333.3, −0.4 (the center of the HII region), (Wilson *et al.* 1970; McGee and Newton 1981) result in values of density and emission measure one or two orders of magnitude larger than those obtained from our measurements (see Table 2). This fact can be explained by the same argument given for M17.

By means of the statistical method referred to above, we estimated an average value for the electron temperature of the low-density ionized gas associated to G333.3 of 5200±500 K. We show in Figure 6 $\int T_L\,dv$ versus T_c and the corresponsing straight-line fit.

c) *RCW 74*

Galactic coordinates and other parameters of the observed profiles are shown in Table 4. Some of the profiles are shown in Figure 7. The centroid velocities of most of the profiles are $\simeq -40$ km s^{-1}, with FWHM of $\simeq 35$ km s^{-1}.

We shown the continuum map in Figure 8. We have indicated with X marks the positions where the H166α line was observed. The values of the computed electron temperatures are given in Table 4, ranging from 4500 to 7500 K; The integrated flux density for the extended region associated to RCW 74 of about 110 arcmin diameter is 1400 Jy. Using the formulation of Schraml and Mezger (1969) the obtained values of electron density and emission measure are $\simeq 7$ cm^{-3} and 8.77×10^3 pc cm^{-6}, respectively. The adopted distance is 3.4 kpc and the diameter of the source is $\simeq 112$ pc.

TABLE 4

PARAMETERS CALCULATED FOR DIFFERENT OBSERVED POINTS IN RCW 74

ℓ (°)	b (°)	$\int T_L\,dv$ (K km s^{-1})	T_c (K)	T_e^* (K)
305.0	− 0.5	2.140	6	7400 ± 700
305.0	+ 0.5	3.660	6	4650 ± 450
306.0	0.0	2.420	5	5650 ± 600
305.5	+ 0.5	4.040	8	5481 ± 5500
305.4	+ 0.2	13.00	22	4780 ± 500
305.0	0.0	7.30	12	4660 ± 450
306.0	− 0.5	1.646	3	5100 ± 500
306.0	+ 0.5	0.432	3	–
305.5	− 0.5	2.838	8	7450 ± 750

Again our values of electron density and emission measure are lower than those obtained from H109α line observations by Wilson *et al.* (1970) and H76α ones by McGee and Newton (1981) (cf. Table 2). The same explanation of this difference as given for M17 and G333.3, should also be valid here. By means of the same method we used for M17 and G333.3, we derive an average electron temperature of 4500±450 K for the low density ionized gas associated to RCW 74. The plot of $\int T_L\,dv$ versus T_c is shown in Figure 9, together with the corresponding fitted straight-line.

IV. THERMODYNAMICAL EQUILIBRIUM

In the high emission measure regions, there are important departures from LTE at the frequency of 1.4 GHz. This results in an increment of the recombination

line temperatures, and therefore generally there is an underestimation of the T_e (LTE). For the low density ionized gas ($N_e \cong 1-10\ cm^{-3}$), of lower emission measure, the T_e^* obtained from H166α and 1.4 GHz continuum observations, should differ from the actual temperature by less than 20% (Dyson 1969). On the other hand, Shaver (1980), shows that, for a given emission meas-

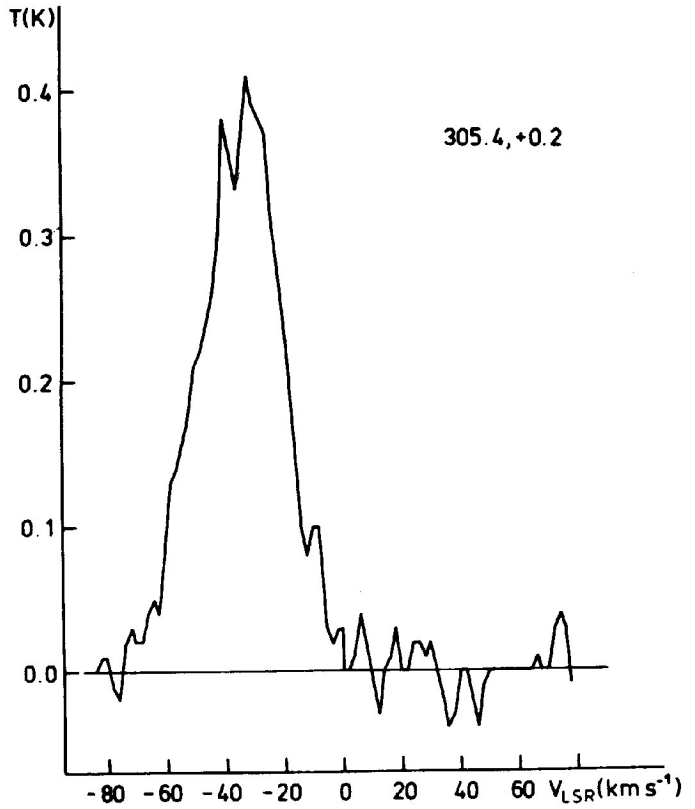

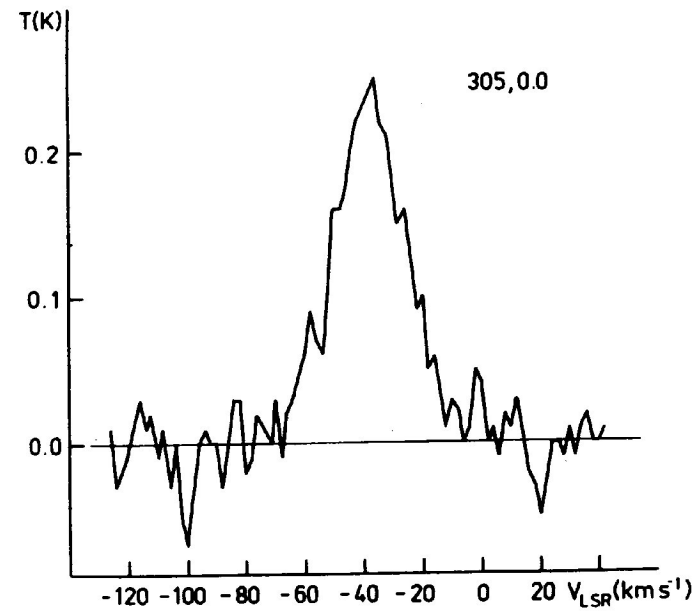

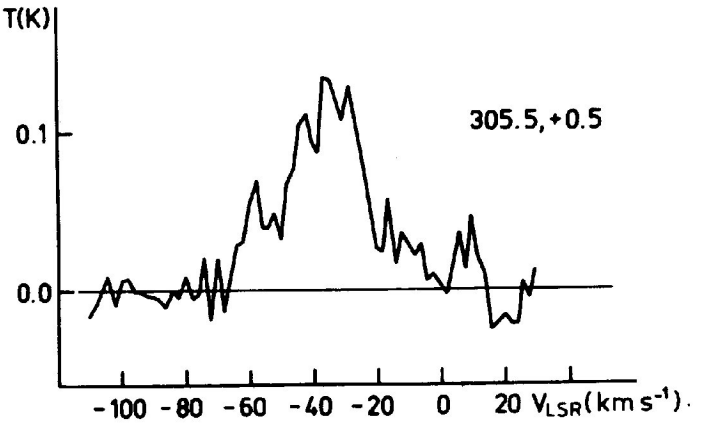

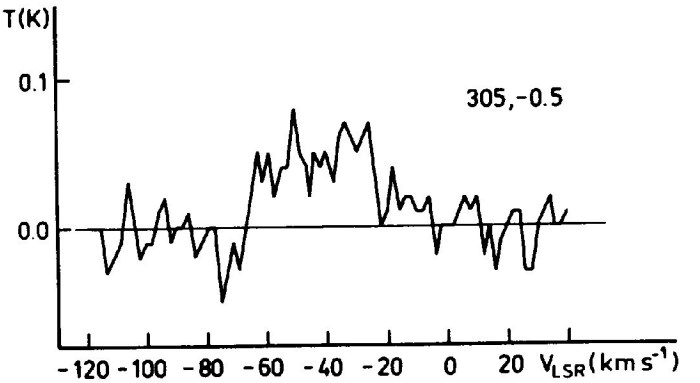

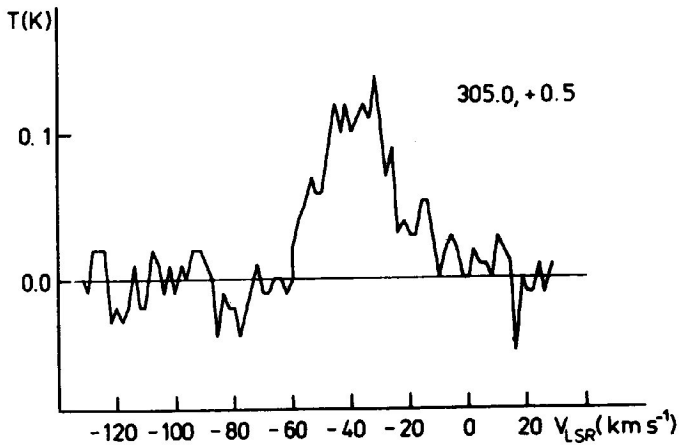

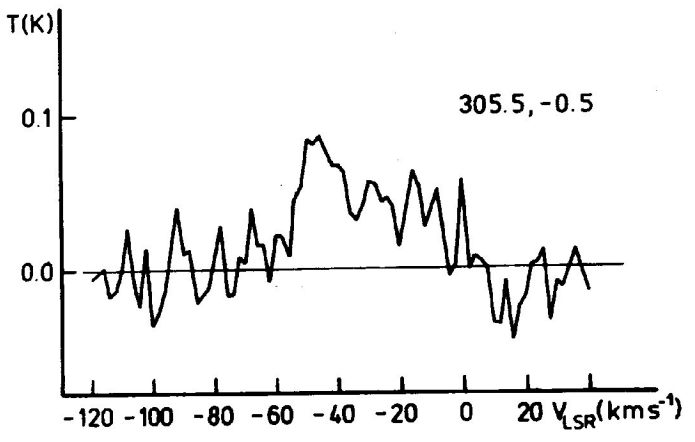

Fig. 7. Some profiles obtained from the H166α observations of the RCW 74 region.

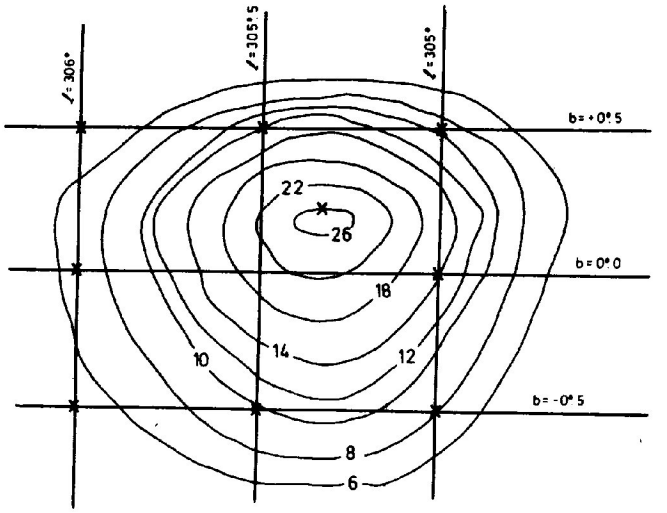

Fig. 8. Continuum map at 1420 MHz of the region associated to RCW 74. The crosses indicate the positions where the H166α line observations were made.

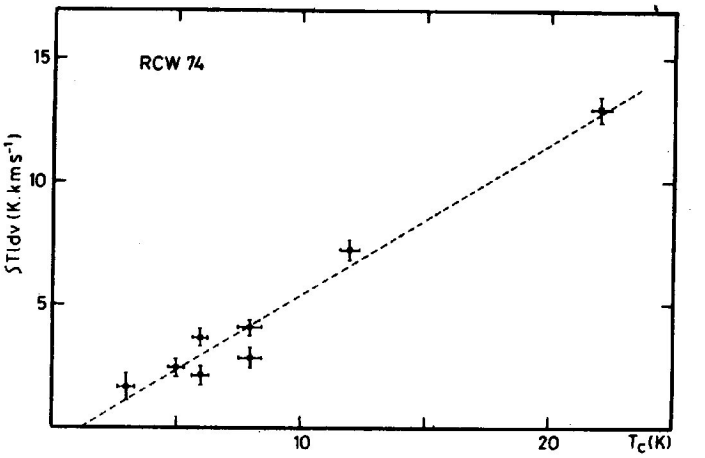

Fig. 9. $\int T_L$ dv versus T_C for RCW 74. The dashed line corresponds to the least squares straight-line fit to the observational results.

ure, there is a unique frequency at which $T_e = T_e^*$. It turns out from his results that at 1.4 GHz and for E.M. = $10^3 - 10^4$ pc cm^{-6}, $T_e \simeq T_e^*$.

In the three regions we observed, the possibility that departures from LTE are present, was investigated through the expression for the ratio of the actual electron temperature T_e, to the value T_e^* obtained by assuming LTE:

$$\frac{T_e}{T_e^*} = \left[b_n \left(1 + \frac{\tau_c}{2} \frac{k T_e}{h\nu} \frac{d \varrho n b_n}{d b_n} \Delta_n \right) \right]^{0.87} \qquad (2)$$

where τ_c is the optical depth for the continuum radiation, b_n is the population departure for the atomic level n. Using the coefficients given by Brocklehurst (1970), we obtained values of $T_e/T_e^* \leqslant 1.2$ for the three regions, as expected.

These results can be explained in two ways either: *i*) there is a compensation between stimulated emission in the low density outer regions by the continuum radiation of the inner core regions and pressure broadening which may be present in the nebulae, or *ii*) the effects of departure from LTE are negligible in our observations and furthermore, pressure broadening is not significant. The latter alternative seems more likely. Pressure broadening does not play a dominant role because the $\Delta\nu_S/\Delta\nu_D$ ratio (Griem 1967) is unimportant for $n > 150$ when the density is $N_e \leqslant 10^3$ cm^{-3}; $\Delta\nu_S$ is the Stark (electron collision) broadened line half-power width, and $\Delta\nu_D$ is the Doppler half-power width.

Therefore, we conclude that the assumption of LTE is a good approximation for the low density gas associated with the three regions.

V. ELECTRON TEMPERATURE VARIATION ACROSS THE H II REGIONS

In Figure 10 we show different electron temperature values obtained for M17, from several radio recombination line observations with different beam sizes (HPBW), as taken from the review by Goudis (1976) as well as from other references (Pedlar and Davies 1972; McGee and Newton 1981; Downes *et al.* 1980; McGee *et al.* 1975). We also include our result (T_e = 5000 K, with a HPBW of 34′). It can be seen from the figure that the temperatures range from 8000 to 4500 K, showing a general trend of decrement as the HPBW increases. In addition, smaller beams correspond generally to higher frequency observations. Two effects ensure that low frequency spectra ($\nu \leqslant 1.4$ GHz) will largely reflect conditions in low-density gas. One of them is the optical

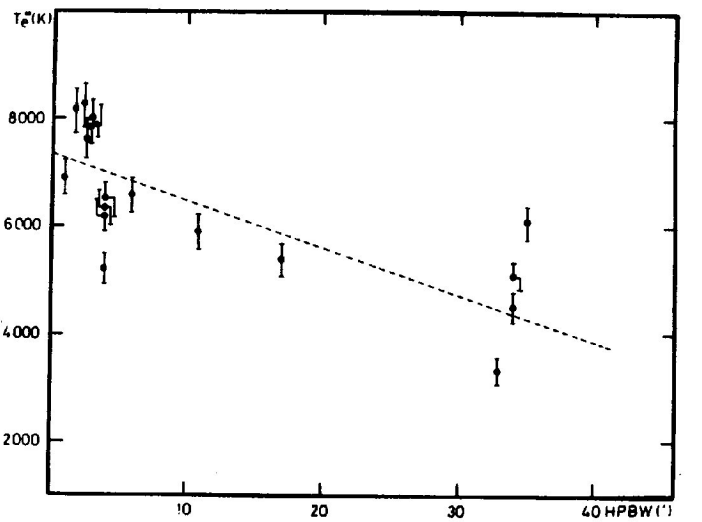

Fig. 10. Plot of electron temperature T_e against beam sizes (HPBW), as obtained from various radio recombination line observations of M17. The dashed line corresponds to the least squares straight-line fit to the observational results.

depth in the continuum for ionized gas, which at the frequency of 1.4 GHz is greater than unity when the emission measure is $> 10^6$ pc cm^{-6}. The second effect arises from impact broadening of the line in dense regions. At 1.4 GHz this broadening will significantly decrease peak line temperatures when $N_e > 1000$ cm^{-3} (Lockman 1976). At high frequencies ($\nu \geqslant 5$ GHz) the observed spectra will be dominated by regions of high N_e, that is to say it will reflect conditions of denser gas.

Therefore, the presence of a variation of the electron temperature with the density in the nebula is apparent. This effect (decreasing electron temperature with decreasing density) has been considered by Pedlar (1980), and Garay and Rodríguez (1983) by comparing electron temperatures of low density and high density H II regions. Low density H II regions are in general cooler than high density ones, due to the lack of collisional de-excitation, that inhibits cooling. In our analysis, we considered the temperature variation across the same region. In this case, there are no effects due to the galactic temperature gradient with the galactocentric distance. Therefore, a model of a hot and high density central region and a low density and cooler envelope, is suitable for describing at least M17.

VI. STAR FORMATION

Compact H II regions expand, and, as their size increases their density and central emission measure decreases. Expansion of the H II regions continues, until they achieve pressure equilibrium with the surrounding neutral gas, or until the ionizing O stars move off the main sequence. Once the electron densities have decreased to some 10 cm^{-3}, they form extended low density H II regions, with low surface brightness, which are difficult to observe at high radio frequencies. However, the free-free emission from a diffuse region, is easily observable with low angular resolution at decimeter wavelengths. The Lyman photon flux required to maintain the radio H II region is provided by O stars. For determining N_c, the Lyman photon production rate in the H II region, we make use of the measured radio flux density S_ν of the free-free emission and of the known distance. The relation between radio luminosity and N_c (Mezger, Smith, and Churchwell 1974) is given by the equation:

$$N_c = 4.76 \times 10^{48} \left(\frac{T_e}{K}\right)^{-0.45} \left(\frac{S_\nu}{Jy}\right) \times \left(\frac{\nu}{GHz}\right)^{-0.1} \left(\frac{r}{kpc}\right)^2 \quad (3)$$

where T_e is the electron temperature, ν is the frequency in GHz, S_ν is the flux in Jy and r is the distance in kpc. We assume the He/H abundance is zero. The results are shown in Table 5.

TABLE 5

THE THREE OBSERVED REGIONS, TOGETHER WITH THEIR FLUXES AND THE CORRESPONDING VALUES OF LYMAN PHOTON FLUX

Region	Distance from the Sun (kpc)	S_ν (Jy)	N_c (Low Density) (ph s^{-1})	N_c (High Density) (ph s^{-1})
M 17	2.3	675	3.7×10^{50}	5.4×10^{50}
G333.3	3.9	1500	2.3×10^{51}	6.3×10^{50}
RCW 74	3.4	1400	1.8×10^{51}	1.4×10^{51}

Since the lifetime of the H II region is relatively short (Osterbrock 1974), we can assume that the stars are on the Zero Age Main Sequence (ZAMS) and with their spectral types according to some initial mass function. Identifying mass with photon flux by using the total luminosity of ZAMS stellar models and the relation of Panagia (1973), between N_c and luminosity, we may calculate the total mass of ZAMS stars associated with a certain Lyman flux.

In each region, we have two different star formation scenarios, one being earlier (high density gas) than the other one (low density gas). We calculated the Lyman flux for the three regions using the parameters obtained from our observations (see Table 5). Comparing these fluxes with those obtained from high frequency determinations (Smith, Bierman, and Mezger 1978), there are no significant differences. That implies the presence of about the same masses of ZAMS stars ionizing both the low and high density gas. Alternatively, it is conceivable that the ionizing cluster is one and the surrounding gas was already in a core-halo distribution. That would be another possibility, different from the assumption of two distinct star formation scenarios.

VII. COMMENTS

We have observed extensively the three H II regions M17, G333.3 and RCW74, in the H166α line and 1.4 GHz continuum. From the observations we derived physical parameters (electron temperature, density and emission measure) corresponding to the low density ionized gas associated to the regions (as was explained above).

On the other hand, from Table 2, it becomes evident that the observations of the higher frequency radio recombination lines, carried out with smaller beams by other authors, supply the physical parameters (essentially electron density and emission measure), corresponding to the denser gas near the center of the nebula. The combined results (at high and low frequencies) are compatible with the description of the relatively extended H II regions as consisting roughly of a small compact region of gas embedded in an extended ionized gas envelope of lower density, as shown in previous papers (Cersosimo 1982; Cersosimo, Azcárate, and Colomb

1984) and studied in more detail for the 30 Doradus nebula (Cersosimo and Loiseau 1984). The conclusion is that observations at a low frequency, such as H166α line, are suitable for obtaining the physical parameters of the lower density ionized gas.

In addition, we have found an electron temperature gradient across M17, which we consider as being due to the variation of temperature with electron density (Pedlar 1980). The values of the electron temperature which we have obtained for the three regions ($\simeq$ 5000 K) are characteristic of low density ionized gas (Pedlar 1980; Cersosimo *et al.* 1984).

We wish to thank the technical staff of the Instituto Argentino de Radioastronomía. We are grateful to Dr. W.G.L. Poppel for his critical reading and useful discussion of the paper. We also thank Mrs. M. Trotz for making the drawings and Miss P. Hurrell for typewriting the tables. We thank the referee for his useful suggestions to improve the paper.

REFERENCES

Brocklehurst, M. 1970, *M.N.R.A.S.*, **157**, 179.
Brand, J. *et al.* 1984, *Astr. and Ap.*, **139**, 181.
Batty, M.J. 1974, *M.N.R.A.S.*, **168**, 37P.
Cersosimo, J.C. 1982, *Ap. (Letters)*, **22**, 157.
Cersosimo, J.C., Azcárate, I.N., and Colomb, F.R. 1984, *Ap. (Letters)*, **24**, 1.
Cersosimo, J.C. and Loiseau, N. 1984, *Astr. and Ap.*, **133**, 93.
De Graauw, T. *et al.* 1981, *Astr. and Ap.*, **102**, 257.
Downes, D., Wilson, T.L., Bieging, J., and Wink, J. 1980, *Astr. and Ap. Suppl.*, **40**, 379.
Dyson, J.E. 1969, *Ap. and Space Sci.*, **4**, 401.
Elliot, K.J. and Meaburn, J. 1975, *Ap. and Space Sci.*, **35**, 81.
Elmegreen, B.G. and Lada, C.J. 1976, *A.J.*, **81**, 1089.
Garay, G. and Rodríguez, L.F. 1983, *A.J.*, **226**, 263.
Genzel, R. and Downes, D. 1977, *Astr. and Ap. Suppl.*, **30**, 145.
Gillespie, A.R. *et al.* 1977, *Astr. and Ap.*, **60**, 221.
Goudis, C. 1976, *Ap. and Space Sci.*, **39**, 273.
Griem, H.R. 1967, *Ap. J.*, **148**, 157.
Gull, T.R. and Balick, B. 1974, *Ap. J.*, **192**, 63.
Hart, L. and Pedlar, A. 1976, *M.N.R.A.S.*, **176**, 135.
Hart, L. Azcárate, I.N., Cersosimo, J.C., and Colomb, F.R. 1983, in *Surveys of the Southern Galaxy*, eds. W.B. Burton and F.P. Israel, D. Reidel Publishing Co., p. 43.
Jackson, P.D. and Kerr, F.J. 1975, *Ap. J.*, **166**, 723.
Knowles, S.H., Caswell, J.L., and Goss, W.M. 1976, *M.N.R.A.S.*, **175**, 537.
Lada, C.J., Dickinson, D.F., and Penfield, H. 1974, *Ap. J. (Letters)*, **189**, L35.
Lada, C.J. 1976, *Ap. J. Suppl.*, **32**, 603.
Lockman, F.J. 1976, *Ap. J.*, **209**, 429.
McGee, R.X. and Newton, L.M. 1981, *M.N.R.A.S.*, **196**, 889.
Meaburn, J. 1977, in *Topics in Interstellar Matter*, ed. H. van Woerden, D. Reidel Publishing Co., p. 81.
Mezger, P.G. and Henderson, A.P. 1967, *Ap. J.*, **147**, 471.
Mezger, P.G., Smith, L.F., and Churchwell, E. 1974, *Astr. and Ap.*, **32**, 269.
Moroney, M.J. 1951, *Facts from Figures*, (London: Penguin Books), p. 135.
Panagia, N. 1973, *A.J.*, **78**, 229.
Pedlar, A. 1980, *M.N.R.A.S.*, **192**, 179.
Pedlar, A. and Davis, R.D. 1972, *M.N.R.A.S.*, **159**. 129.
Osterbrock, D.E. 1974, in *Astrophysics of Gaseous Nebula*, (San Francisco: Freeman and Co.), p. 210.
Robinson, B.J. *et al.* 1984, *Ap. J. (Letters)*, **283**, L31.
Schraml, J. and Mezger, P.G. 1969, *Ap. J.*, **156**, 269.
Shaver, P. 1980, *Astr. and Ap.*, **91**, 279.
Smith, L.F., Bierman, P., and Mezger, P.G. 1978, *Astr. and Ap.*, **66**, 65.
Thronson, H.A., Jr. and Lada, C.J. 1983, *Ap. J.*, **269**, 175.
Whiteoak, J.B. and Gardner, F.F. 1974, *Astr. and Ap.*, **37**, 389.
Wilson, T.L., Mezger, P.G., Gardner, F.F., and Milne, D.K. 1970, *Astr. and Ap.*, **6**, 364.

I.N. Azcárate, J.C. Cersosimo, and F.R. Colomb: Instituto Argentino de Radioastronomía, Casilla de Correos No. 5, Villa Elisa, 1894 Argentina.